

Characteristics of Extreme Precipitation Events over the Arctic Region

Caitlin M. Mc Shane

Geography Departmental Honors Thesis

University of Colorado at Boulder

Defended April 4, 2016

Thesis Advisor

Dr. Mark C. Serreze | Department of Geography

Defense Committee:

Dr. Mark Serreze | Department of Geography

Dr. William Travis | Department of Geography

Dr. John Cassano | Department of Atmospheric Science and Oceanic Studies

Table of Contents

Abstract..... 3

1.0 Introduction..... 4

 1.1 *Water Vapor*..... 5

 1.2 *Spatial Variability of Precipitation*..... 6

 1.2.1 *Storm Tracks*..... 6

 1.2.2 *Central Arctic Ocean and Continents*..... 7

 1.3 *Atmospheric Variability in the Arctic*..... 7

 1.4 *Sea Ice Cover* 8

2.0 Data and its Preparation 9

 2.1 *Station Precipitation Data*..... 9

 2.2 *Atmospheric Reanalysis Products* 10

3. Spatial Pattern of Extremes..... 11

4.0 Case Study Analysis Results..... 11

 4.1 *Robertson Lake NU, Canada* 12

 4.2 *Qikiqtarjuaq A, Canada*..... 14

 4.3 *Kelly Station, Alaska* 16

5.0 Trends Analysis Results 18

6.0 Discussion 20

7.0 . Conclusion..... 22

8.0 References..... 23

Characteristics of Extreme Precipitation Events over the Arctic Region

Caitlin M. Mc Shane

mcschanec@colorado.edu

Abstract

The Arctic (the region poleward of 65°N) is experiencing an outsized warming relative to the rest of globe, accompanied by sharp reductions in sea ice extent. Has this been attended by changes in extreme weather events? In this study, the spatial characteristics and recent trends of extreme daily precipitation events across the Arctic are examined using station records from the National Climatic Data Center, The Norwegian Meteorological Institute and other national sources. The focus is on the period 1979-2014. Extreme events for each of the 145 stations selected for analysis, based on record length and data quality, are defined as those within the top 1% of each station's statistical distribution. The spatial distribution of the size of the 1% event broadly follows the spatial pattern of annual precipitation. For stations in Iceland, Svalbard and coastal Norway, which are influenced by Atlantic moisture sources, the 1% event size ranges from 14 to 25 mm. This contrasts sharply with polar desert sites in the Canadian Arctic Archipelago and many locations along the Siberian coast that have values from only 3-10 mm. Case studies demonstrate coherent relationships between extremes and the influence of both synoptic-scale and local uplift mechanisms, and the availability of water vapor. When the Arctic region is assessed as a whole, the frequency of extreme events shows a slight positive trend. However, regional analysis reveals areas of both positive and negative trends, with the sign of trends dependent on region, season and month.

1.0 Introduction

Extreme precipitation events can have a significant impact on human societies. The cost of human life and damage to infrastructure can be devastating and impose a great economic burden on affected communities. Studying potential increases in extreme precipitation events as a result of increasing global temperatures will help prepare communities to mitigate the potentially calamitous effects of such change. There is strong evidence for increases in precipitation extremes across the contiguous United States and other parts of the world. Recently, significant attention has been given to changes in extratropical cyclone frequency and associated precipitation in response to a warming climate.

The International Panel for Climate Change's (IPCC) 2013 report, *Climate Change 2013: The Physical Science Basis*, indicates that statistically significant increases in cyclone frequency have been observed mainly in North America. Changes in the frequency of extratropical cyclones are of particular import to the Arctic as cyclones are the main avenue by which sensible heat and moisture are transported into the region. Glisan and Gutowski (2014) found that areas of the Arctic associated with low level convergence of moisture tend to be areas prone to extreme precipitation events. Increased occurrence of cyclonic activity may add to the moisture content of the atmospheric column and may lead to stronger extremes as extreme precipitation scales to total column moisture content (IPCC, 2013). Additional moisture in the atmospheric column may also lead to an increase in latent heat release during a precipitation event causing conditional atmospheric instability that encourages storm growth (Saha et al. 2006). Ulbrich et al. (2013) conducted a study that compares the output of the most widely used coupled global climate models and found generally high agreement regarding the latitudinal bands over which cyclone frequency will change. There are strong regional variations in observed trends with notable increases over parts of Asia, the Bering Sea, and the eastern North Atlantic (Ulbrich et al. 2013).

Environmental and climatic changes over the past century have altered the stability of the Arctic region. The Arctic is warming at a much faster pace than lower latitudes, a phenomenon known as Arctic Amplification (AA) (Francis and Vavrus, 2012; Serreze and Barry 2014; Overland et al. 2015). The observed changes in the Arctic's climatic patterns, linked to AA, may offer some insight as to how climate regimes in other parts of the globe may respond in the future. The Arctic is linked to the global climate system through broad-scale atmospheric patterns, which are influenced through a series of complex feedback mechanisms. An energy deficit exists in the polar regions due to the uneven heating of the Earth's surface; this deficit is a key driver of global circulation and plays a major role in energy and moisture transport into and out of the Arctic (McGuire et al. 2006). Increasing horizontal heat and moisture fluxes into the Arctic have been attended by changes in sea level pressure (SLP), sea ice cover, precipitation patterns, hydrology and ocean currents, and lengthening of the melt season (Macdonald et al. 2005). Changes in sea-ice extent are of particular importance to the Arctic system as sea ice variability strongly impacts ocean/atmosphere turbulent fluxes and may also affect atmospheric circulation patterns, such as the North Atlantic Oscillation and Arctic Oscillation (Alexander et al. 2004; Porter et al. 2012; Serreze and Barry 2014). Furthermore, enhanced melt, resulting from the ice-albedo feedback, increases freshwater input into the Arctic Ocean, which has the potential to influence North Atlantic Deep Water (NADW) production and alter global ocean currents (Serreze and Barry 2014). AA has contributed to substantial changes in the region's climate system, however, the complex land-ocean-atmosphere interactions and the high spatial variability within the region make it difficult to quantify these changes.

The Arctic region, defined here as northward of 65°N, is characterized by a highly dynamic climate system that may affect global weather patterns, particularly in the mid-latitudes. Some of the current research investigating the effects of the Arctic on mid-latitude weather shows a strong association between sea ice loss and anomalously cold Asian winters (Hori et al. 2011; Mori et al. 2014). Other studies suggest that AA has diminished the temperature gradient between polar and mid-latitude air masses, in turn reducing the strength of the polar jet stream, which effectively slows the eastward progression of upper-level waves and creates persistent mid-latitude circulation patterns (Francis and Vavrus,

2012; Cvijanovic, et al. 2015; Overland et al. 2015). However, there remains some ambiguity about whether the magnitude of AA has reached upper-level circulation, which is necessary if changes in the jet stream were to occur.

To provide a comprehensive picture of the spatial characteristics of extreme precipitation within the Arctic it is useful to first review the Arctic climate system. The following sections will address (1) the spatial variability in water vapor and precipitation patterns across the various climate regimes within the Arctic, the origins and drivers of these patterns, and their effect on the Arctic's energy balance, (2) the large-scale circulation patterns that dominate the Arctic, especially the AO and NAO, and their effect on precipitation patterns and ice-extent, and (3) the implications of a shrinking sea ice cover in relation to the energy budget and precipitable water, the importance of sea-ice extent, and how declining sea-ice affects atmospheric circulation. Following this background, data sources and methodology are detailed, several case studies are outlined, and main results are discussed.

1.1 Water Vapor

The Arctic is home to several climate regimes, ranging from maritime to polar desert, which are characterized by spatial heterogeneity in orography and proximity to large water bodies (Serreze and Barry 2014). The large spatial variability in the Arctic's physical geography is a driving mechanism of regional precipitation patterns and determines regional variations in precipitation seasonality. While myriad precipitation-generating mechanisms exist, the Arctic, except for its wettest areas, in particular, the southeast coast of Greenland, is a relatively dry, water-limited environment due to the low water holding capacity of the atmosphere (Serreze and Barry 2014). The Clausius-Clapeyron equation defines the (positive) exponential relationship between water vapor saturation and temperature. Recently temperatures have been increasing on a global scale, but particularly north of the Arctic Circle. Increasing the water vapor content of the overlying atmosphere may change the spatial characteristics of regional precipitation patterns within the Arctic.

Atmospheric transport of water vapor into the Arctic is a crucial part of the Arctic's energy budget. The horizontal vapor flux convergence brings in a significant amount of energy via the North Atlantic storm track, acting to reduce the large temperature gradient between the equatorial regions and the poles (Serreze and Barry 2014). As surface air temperature (SAT) increases at lower and middle latitudes, atmospheric heat advection increases, bringing substantial latent and sensible heat energy into the Arctic (McGuire et al. 2006). Langen and Alexeev (2004) estimate that nearly half of the observed warming in the Arctic can be attributed to the increased heat flux from lower latitudes. Therefore, the atmospheric eddies that move poleward have greater water vapor concentration and heat content (McGuire et al. 2006; Serreze and Barry 2014), which ultimately adds to the amount of moisture in the Arctic's atmospheric column. Indeed, various studies have found that despite significant heterogeneity through time and space, there are positive trends in water vapor for all seasons in the Arctic (Uppala et al. 2005; Francis and Hunter 2007; Rinke et al. 2009; Screen and Simmonds 2010; Dee et al. 2011; Serreze et al. 2012). Because large amounts of energy (2.25 MJ g^{-1} at 0°C) are required to change water from a liquid to a gas and this energy must be conserved, an equal amount of energy is released upon condensation. Due to the conservation of energy and that water vapor is a greenhouse gas, water vapor can dramatically affect the energy budget of a climate system and has the potential to increase event intensity.

Water vapor is the most abundant greenhouse gas that maintains the earth's natural greenhouse effect (Held and Soden 2000; Gusakova and Karlin 2014; Serreze and Barry 2014) and a series of positive feedbacks are associated with increasing the concentration of water vapor in the atmospheric column. Water vapor amplifies the effects of other greenhouse gases that have longer residence times and increases climate sensitivity (Held and Soden 2000). As discussed previously, rises in SAT further increase the water holding capacity of the atmosphere, and thus, the water vapor-SAT cycle is perpetuated (Held and Soden 2000; McGuire et al. 2006; Serreze and Barry 2014). Increased SAT has a large impact on sea ice melt which triggers the ice-albedo feedback and ultimately increases the amount of absorbed solar radiation at the surface, in turn increasing evapotranspiration (ET) and convective type air movement (Held and

Soden 2000; McGuire et al. 2006; Serreze and Barry 2014). Changes in such important climate parameters may alter the local climate's annual precipitation patterns.

1.2 Spatial Variability of Precipitation

The Arctic can generally be classified into two distinct regions in terms of the spatial distribution of precipitation: areas that are strongly influenced by storm tracks and areas that fall outside of major storm track influence. Temporal patterns of precipitation within these regions are driven by the availability of water vapor, which varies from summer to winter. Such variability in precipitable water determines the season in which a given region will experience its precipitation maximum.

1.2.1 Storm Tracks

The Arctic climate system is affected by two primary storm tracks: The North Atlantic storm track and the East Asian storm track. The region influenced by the North Atlantic storm track, in particular, the southeast coast of Greenland, sees the highest precipitation totals in the Arctic locally upwards of 2000 mm annually. This area lies along the polar jet stream that marks the boundary between polar and sub-tropical air masses resulting in a zone of enhanced baroclinicity and a semi-permanent center of action called the Icelandic Low (Serreze et al. 1997). At its maximum elevation the ice sheet is 3,000 meters above sea level (Schuenemann et al. 2009). The presence of the ice sheet not only forces orographic uplift of poleward moving air parcels (accounting for the high totals along the southeast coast of Greenland), but the cold air over the ice sheet further enhances the baroclinicity of the region (Serreze and Barry 2014). Warm air masses moving toward the pole originate over waters with much higher sea surface temperature (SST) and have higher precipitable water content than air masses that originate from the north. The transfer of atmospheric energy is proportional to the size of the temperature gradient between the equatorial regions and the poles. Thus, the North Atlantic storm track is most active during the winter months. The general circulation strengthens as a result of the enhanced baroclinicity, which increases cyclone frequency and the poleward transfer of heat and moisture into the region (Schuenemann et al. 2009). As summer approaches and the basic horizontal temperature gradient weakens, the Icelandic low weakens, cyclone frequency decreases overall and the horizontal vapor flux convergence into the Arctic is reduced.

The driving mechanisms of the East Asian storm in the Pacific track are similar in nature to those in the North Atlantic storm track; both tracks show areas of maximum cyclone activity manifested as semi-permanent low pressure centers (the Icelandic and Aleutian Lows), which are located down stream of major mid-tropospheric stationary troughs (Serreze and Barry 2014). The areas characterized by the East Asian storm track also experience winter precipitation maxima as the Aleutian Low strengthens and advects warm, moist air from lower Pacific latitudes (Gong and Ho 2002; Nakamura et al. 2002; Serreze and Barry 2014). Additionally, the cold Siberian High exerts a significant influence on the hydrologic cycle (Gong and Ho 2002). Positive pressure anomalies associated with the Siberian High result in anomalously low air temperatures over Eurasia and suppression of the hydrologic cycle in the Siberian region (Gong and Ho 2002; Nakamura et al. 2002; Serreze and Barry 2014). Very low SATs over the Eurasian continent during the winter, resulting from a strengthened Siberian High, help to enhance baroclinicity between the comparatively warm waters of the North Pacific and cold land surface. Storms that originate along the coast of Japan and Siberia travel poleward and feed into the Aleutian Low, which peaks in strength during the winter (Ludlum 1998). Winter storms generated in the Pacific rarely migrate into the central Arctic as cyclones are frequently blocked by the Beaufort High, which reaches its highest pressure during this time (Gong and Ho 2002; Nakamura et al. 2002). Thus, the East Asian storm track exerts the most influence on the Pacific side of the Arctic.

1.2.2 Central Arctic Ocean and Continents

In the Central Arctic Ocean (CAO) and land areas that are generally removed from the influence of winter cyclones, winters are dry. Winter precipitation totals over large tracts of eastern Eurasia, northern Alaska, northern Canada, and the CAO average between 10-20mm. While the Atlantic and Pacific sectors generally have the highest precipitation totals for the summer months, precipitation is at its annual maximum for the CAO and most land areas (Serreze and Barry 2014). Summer precipitation maxima in these areas are driven by several processes including convection (over land only), increased cyclone activity, and the summer Arctic Frontal Zone.

During the summer, solar radiation absorbed at the surface increases significantly over land areas promoting snow melt, ET, and increased SATs. Higher rates of ET over land areas and strong surface heating increase the occurrence of convective type precipitation (Serreze and Barry 2014). Gong and Ho (2002) showed that there is remarkable surface warming associated with a weakened Siberian High. Over Eurasia, the Siberian High weakens considerably as snow cover declines, which in turn decreases the stability of the lower troposphere and encourages greater precipitation (Gong and Ho 2002; Serreze and Barry 2014). Receding snow cover and reductions in sea ice cover from summer melt cause strong differential heating between the CAO and snow-free land causing an eastward shift in the Urals Trough (Serreze and Barry 2014). These heating contrasts enhance coastal baroclinicity, which is further sharpened by local orography (i.e., the Urals mountain range) and increases frontal frequencies over Alaska and Eurasia. Similarly, increased frontal frequencies along the Canadian coast are also observed in summer due to the differential heating between the CAO and snow-free land (Serreze and Barry 2014). The contribution of this Arctic Frontal Zone to annual precipitation over coastal land areas is significant. Serreze and Barry (2014) found that at 140° E (Eurasian frontal zone) more than 60% of annual precipitation falls in the summer and where the Alaskan summer frontal zone is prominent more than 50% of annual precipitation falls in the summer.

The summer maximum in precipitation over the CAO largely reflects an increased frequency of cyclone activity. This is due both to cyclones that penetrate into the region generated along the North Atlantic storm track and those originating in Eurasia, including where the Arctic frontal zone is best expressed (Serreze and Barry 2014). Precipitation totals over the CAO peak in September and can reach 30 mm.

1.3 Atmospheric Variability in the Arctic

Several modes of atmospheric variability affect the Arctic. These teleconnections operate on time scales ranging from weeks to months to years, and each exerts some influence on local and regional climates. The Pacific sector is dominated by the Pacific Decadal Oscillation (PDO) which is defined as the leading component of SST variability in the North Pacific (Mantua et al. 1997; Serreze and Barry 2014). The positive (negative) PDO is characterized by anomalously high (low) SST between the North Pacific coast and low (high) SST in the interior North Pacific, and has been linked to variability in sea level pressure (SLP) manifested in the strength of the Aleutian Low (Serreze and Barry 2014). The phase of the PDO has a significant impact on SAT anomalies over Alaska and local precipitation patterns (Serreze and Barry 2014).

The North Atlantic is dominated by the North Atlantic Oscillation (NAO). The NAO is characterized by the covariance between the strength of the Icelandic Low and the Azores high (Serreze and Barry 2014), manifested as a seesaw pattern in precipitation and temperature between Greenland and Northern Europe (Cohen and Barlow 2005). In its positive phase the Icelandic Low and Azores high are relatively strong. Conversely, when these centers of action are weak, the NAO is said to be in its negative phase (Serreze and Barry 2014). During the NAO positive phase, strong westerlies are observed over the North Atlantic extending into Europe, and during the negative phase of the NAO these westerlies are significantly reduced (Wanner et al. 2001). Associated with each phase of the NAO are varying spatial-temporal patterns

in precipitation, SAT, moisture transport, cyclone activity, SST, and ocean heat transport (Wanner et al. 2001; Serreze and Barry 2014).

The NAO is a primary source of seasonal and decadal variability in Northern Hemisphere circulation (Wanner et al. 2001) and it is a significant contributor to the variance in SLP (Serreze and Barry 2014). In the NAO's positive phase, there is increased cyclone activity along the North Atlantic sector (Serreze and Barry 2014). Cyclones that penetrate deeper into the Arctic region generate greater amounts of precipitation in the area through frontal uplift (McGuire et al. 2006; Serreze and Barry 2014). The NAO has shown a weak response to changes in the sea ice margin. Francis et al. (2009) find that summers with reduced sea ice extent are followed by autumn and winters where the NAO was neutral or negative, suggesting an impact on precipitation as summer sea ice extent recedes.

The Arctic Oscillation (AO) is characterized by SLP variability over the Icelandic Low and weaker centers of action over the North Atlantic and North Pacific (Zhao et al. 2010; Serreze and Barry 2014). The AO encompasses the two centers of action which define the NAO in addition to a third center of action in the North Pacific (Zhao et al. 2010). The covariance in SLP between the Icelandic Low and Azores high extends to the North Pacific; when SLP is low over the Arctic, SLP is high in the North Atlantic and North Pacific (Serreze and Barry 2014). Spatial patterns in associated weather anomalies are similar to those associated with the NAO, however, there are two primary differences between the AO and NAO. There is a stronger correlation (positive) between SAT and the AO over Northern Eurasia and a stronger (negative) correlation between SAT and the AO over southern Alaska (Serreze and Barry 2014). While there are several other important teleconnections that contribute to the Arctic's climate system, the NAO, AO, and PDO exert a heavy influence on local precipitation and are therefore the primary teleconnections discussed in this paper.

1.4 Sea Ice Cover

Changes in Arctic sea ice cover have been shown to impact climates as far away as the tropics (Semmler et al. 2012). A primary function of sea ice cover in the Arctic is to regulate energy exchanges between the ocean and atmosphere (Francis et al. 2009). Arctic sea ice extent also exerts a strong influence on surface wind, and the stratification of the upper ocean (Bhatt et al. 2008). Sea ice extent exhibits similar variability to that of the NAO/AO on decadal and longer timescales, however, there is also variability on seasonal timescales driven by changes in the local climate (Bhatt et al. 2008). Using a general circulation model, Magnusdottir et al. (2004) found that changes in sea ice extent had a significant impact on the location of the North Atlantic Storm Track and large scale circulation suggesting a subsequent impact on Arctic precipitation.

Various studies have examined ice extent and the effect it has on large scale teleconnections and precipitation patterns. Generally, low sea ice extent is associated with positive SAT anomalies that are most pronounced between December and March (Murray and Simmonds 1995; Honda et al. 1996; Parkinson et al. 1999; Alexander et al. 2004). As sea ice extent declines, the ocean-to-atmosphere turbulent heat flux increases (Porter et al. 2012; Serreze and Barry 2014). Additionally, increasing surface melt and open water further the response of the albedo-temperature feedback resulting in higher observed SAT (McGuire et al. 2006). Enhanced ocean to atmosphere heat fluxes and rising SAT, resulting from declining sea ice extent, increase the water vapor content of the atmospheric column and potentially influence large scale atmospheric circulation patterns (Alexander et al. 2004; Serreze and Francis 2006; Francis et al. 2009; Porter et al. 2012). Using the Community Climate Model, Alexander et al. [2004] found a strong correlation between reduced (enhanced) precipitation and evaporation over areas with more (less) sea ice. Sea ice variability has been linked to variability in precipitation throughout the Arctic and may force changes in atmospheric teleconnections, including negative responses in the Atlantic sector (less sea ice means a weaker NAO) and positive responses in the Pacific sector (less sea ice means the PDO index is more positive) (Alexander et al. 2004; Deser et al. 2007; Bhatt et al. 2008; Francis et al. 2009).

2.0 Data and its Preparation

Use was made of daily Arctic precipitation records from several sources. There are significant hurdles to overcome when using Arctic station data, such as measurement bias and incomplete records. While no correction algorithms were used to mitigate error, strict quality control was employed to screen out spurious data. To provide insight into the atmospheric patterns associated with precipitation extremes in three case studies, use was made of atmospheric circulation and precipitation fields from two atmospheric reanalyses: 1) the National Centers for Environmental Prediction Climate Forecast System Reanalysis (NCEP/CFRS) (Saha et al. 2010) and 2) the National Center for Environmental Prediction/National Center for Atmospheric Research (NCEP/NCAR) (Kalnay et al. 1996).

2.1 Station Precipitation Data

Daily precipitation records were gathered from 145 gauging stations distributed across Arctic land areas and islands from multiple sources. **Figure 1** shows the spatial distribution of the selected stations. The majority of the records used in this study were obtained from the Global Historic Climate Network (GHCN) database maintained by the National Oceanic and Atmospheric Administration (NOAA). Data from several other sources, such as the Norwegian Meteorological Institute (NMI), National Snow and Ice Data Center (NSIDC), and National Resources Conservation Service (NRCS), provided roughly half of the data records combined. The GHCN database supplied records from 78 stations covering Canada, Greenland, Iceland, Norway, Russia, Svalbard and Alaska. The NSIDC supplied records from 58 gauging stations covering areas of Svalbard and Russia. Similarly, NMI supplied records from 10 gauging stations covering areas of Svalbard and Northern Norway. The NRCS supplied records from eight stations covering Northern Alaska. Note that there is no systematic precipitation monitoring program over the central Arctic Ocean.



Figure 1: Map of the spatial distribution of the gauging stations used for study

| GHCN Quality Flags | |
|--|---|
| • D = failed to duplicate check | • O = failed climatological outlier check |
| • G = failed gap check | • R = failed lag range check |
| • I = failed internal consistency check | • S = failed spatial consistency check |
| • K = failed strea/frequent value check | • T = failed temporal consistency check |
| • L = failed check on length of multiday | • W = temperature too warm for snow |
| • M = failed megaconsistency check | • X = failed bounds check |
| • N = failed night check | • Z = flagged as a result of an official Datzilla investigation |

Table 1: Table of the data quality flags used by the GHCN database

To be included, station records must span at least 20 years over the period 1979-2015 with a reasonable distribution of valid data across the study time period. Corrections for gauge undercatch were not accounted for in this study due to the difficulties in obtaining the atmospheric and surface conditions at the time of measurement. Data was selected based on three primary criteria: availability, quality, and length of the station records. After data for a gauging station was obtained, additional considerations were made during the data cleaning process.

Table 1 lists the various quality flags that were found within the data. All observations that had an associated quality flag were eliminated and

replaced with a missing value. The only quality flag for which the observation was not eliminated was the 'climatological outlier flag'. Removing these observations would have reduced the incidence of potentially valid extreme precipitation events from the data records, as this quality flag marked that the measurement had some probability of being erroneous because it was simply an exceptionally high value. Extreme precipitation events are low probability events by nature and removing these data values may have ultimately introduced greater bias into the analysis.

There are many issues surrounding the collection of precipitation data and these are particularly pronounced in the harsh Arctic environment. The primary issues include gauge undercatch, inadequate network density, and incomplete data records (Serreze and Barry 2014). Furthermore, data records may be difficult to obtain due to the lack of international cooperation and a centralized location to house compiled records.

Gauge undercatch is one of the largest sources of error. Undercatch refers to the inability of gauging stations to collect 'true' precipitation values due to these severe environmental conditions in the Arctic. Persistent winds cause drifting snow and create serious biases in gauge measurements (Serreze and Barry 2014). Yang et al. (2001) note that wind speed is the most important variable that influences gauge catch efficiency, and it is estimated that error can reach 50-100% in environments such as the Arctic (Serreze and Barry 2014). As with most elements in the Arctic, wind speed displays high spatial variability, the averages range from 4 m s^{-1} over the central Arctic Ocean to 12 m s^{-1} in areas such as the Barents Sea, Bering Sea, and southeastern Greenland. However, gales are common and can last for several days bringing wind speeds up to 45 m s^{-1} in some areas. Attempts to correct for these biases are imperfect and require information on the type of gauge being used, wind velocities, and the conditions of the site at the time of measurement (Serreze and Barry 2014). This type of information was largely unavailable for the gauging stations used in this study and no corrections were attempted.

The limited number of gauging stations in the Arctic results in poor spatial sampling of precipitation. Installation and maintenance of gauging stations is expensive due to the harsh climate. Budget cuts have forced the closure of many gauging stations across the region, limiting data that extends significantly into the 21st century. While daily records exist for numerous gauging stations, the continuity of an individual station's record may be patchy. Some stations have missing values that extend from days to years at a time, making it difficult to study local trends in extreme precipitation. Another difficulty is that data are scattered between archives. Oftentimes there is significant overlap between databases, and station records may be duplicated under different station identification tags. Time stamps, indicating the date and time that a measurement is taken, differ from country to country, which can affect the day a precipitation event appears to have happened. For example, the time stamp used by the Norwegian Meteorological Institute begins and ends at 1800 on each day, potentially moving a precipitation event a day forward.

2.2 Atmospheric Reanalysis Products

The starting year, 1979, marks the advent of the modern satellite record which is when the two atmospheric reanalysis start providing coverage. CFSR and NCEP/CFSR reanalyses are numerical weather prediction (NWP) models used for short to medium range weather forecasting (Serreze and Barry 2014). NWP accuracy is heavily dependent on the correct representation of initial atmospheric conditions, and for this reason there is an ongoing process to 'reset' these models to true conditions via data assimilation techniques (Serreze and Barry 2014). Satellite observations represent key sources of the necessary data (primarily information on tropospheric temperature and humidity). While it is tempting to accept the output of such models as 'truth' there are definitive biases produced by these reanalyses resulting from both deficiencies in model physics and difficulties of setting accurate initial atmospheric conditions. As mentioned, use is made of the reanalysis data (circulation fields and precipitation) in case studies.

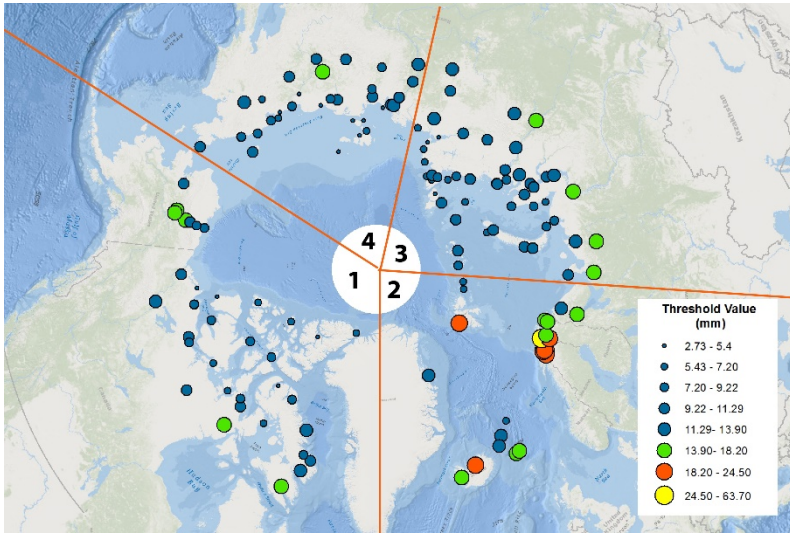


Figure 1: Map depicting individual station threshold values and regions used for analysis

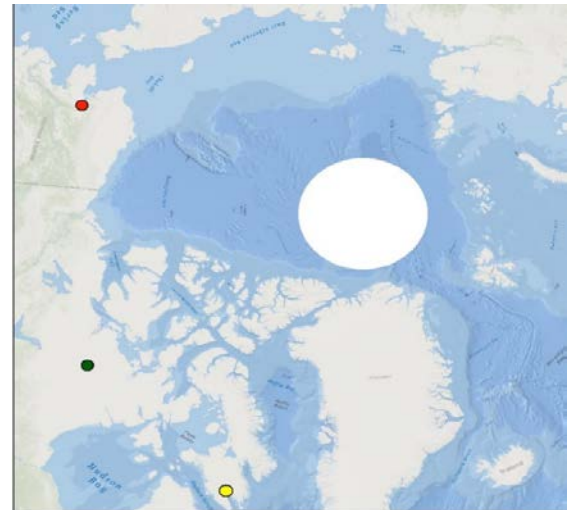


Figure 3: Map depicting the location of the stations used for case study analysis. Kelly station-upper left corner in red; Nunavut station middle in green; Baffin Island station lower left in yellow

3. Spatial Pattern of Extremes

This study’s aim is to use daily precipitation records to examine extreme precipitation events in the Arctic since 1979 and assess whether there have been changes in the frequency and intensity of extreme events since that time. To examine extreme precipitation events, it is necessary to first formally define such events. The nature of extremes implies a significant deviation from the sample mean, therefore, only events in the 99th percentile (top 1%) were considered extreme events. This will henceforth be termed the threshold value. The frequency and intensity of extreme events were considered on several time scales: annual, seasonal, and monthly.

To help set the stage for the analysis of case studies and trends patterns, **Figure 2** provides a graduated symbol map depicting individual station threshold values. The map highlights the variation in precipitation around the Arctic. In dry areas, far from ocean moisture sources, an extreme event may be no larger than 2 mm. As expected, the largest threshold values are found in the Atlantic region influenced by the North Atlantic cyclone track where water vapor is more abundant and where precipitation-generating mechanisms are strong. Based on regional similarities between threshold values, the Arctic was partitioned into four regions (also shown in Figure 2) to facilitate a more localized analysis.

4.0 Case Study Analysis Results

Before continuing, it is useful to examine a few case studies. This section investigates the largest extreme precipitation events recorded at three different stations in different part of the North American Arctic. NCEP/NCAR and CFSR atmospheric reanalyses were used to assess atmospheric conditions and large-scale precipitation patterns at the time of each event. **Figure 3** displays the geographic location of the stations that were investigated.

4.1 Robertson Lake NU, Canada

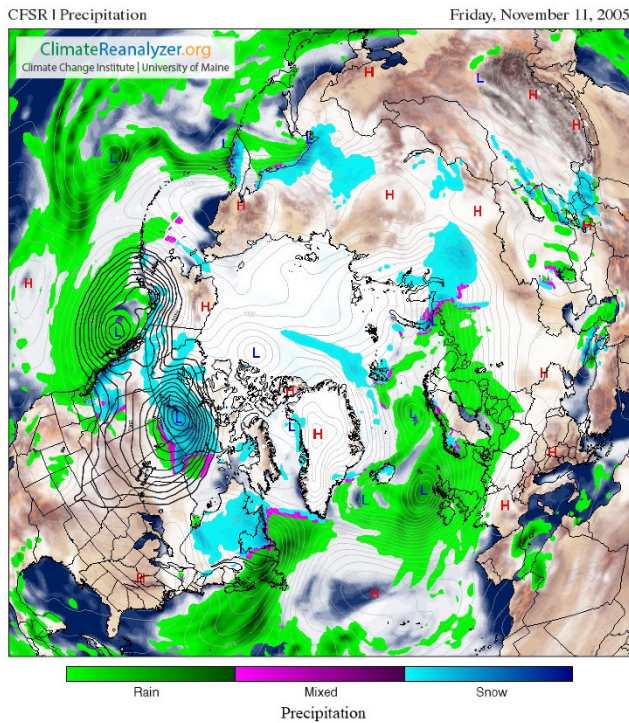


Figure 4: Precipitation fields from NCEP/CFSR for the Nunavut station in central northern Canada darkened contour lines depict SLP

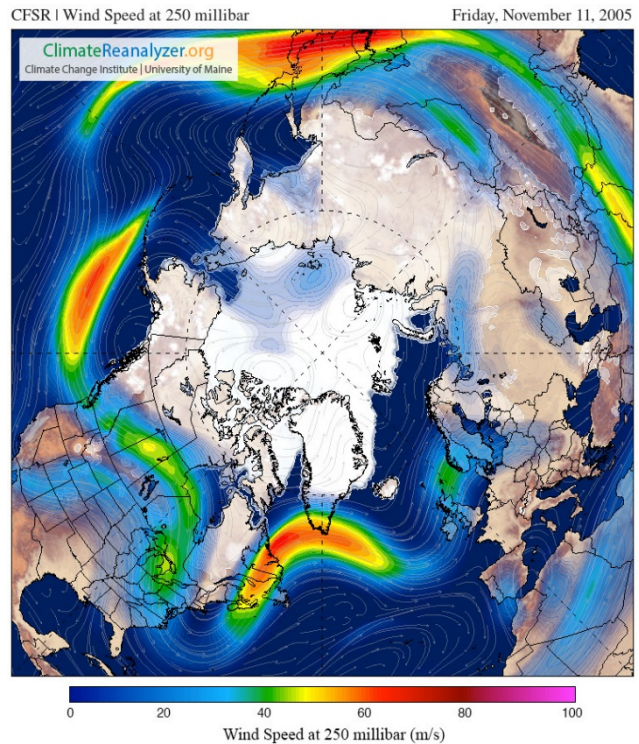


Figure 5: Winds speeds at the 250mb height on November 11, 2005

Robertson Lake station is located within the Keewatin district of southwestern Nunavut territory, Canada. The local climate is strongly continental and is subject to large variations in temperature compared to more marine climates. The region can in turn be categorized into two distinct sub-regions: (1) the Canadian Shield, which includes the mainland and the islands surrounding Hudson Bay, and (2) the Canadian Arctic Archipelago in the north. The Canadian Shield is characterized by hundreds of lakes carved out during the last glacial cycle and a relatively flat topography with an average relief of 30 meters (<http://www.britannica.com/place/Nunavut>). The Nunavut territory is classified as a dry High-Arctic ecoclimate where the annual precipitation ranges from 100-200 mm (Devlin and Finkelstein, 2011). Over the past decade significant changes in extreme precipitation and wind patterns have taken place across the Nunavut territory with multiple record breaking events since 2005 (Hanesiak et al. 2010). The event under investigation at this site started on November 11, 2005 and generated approximately 35 mm of precipitation in a 24-hour timespan, which is in the 99.9th percentile of the station’s record. From fields generated by NCEP/NCAR and NCEP/CFSR reanalysis, it appears that this event was driven by a cyclone that originated over the North Pacific. Considering the atmospheric conditions in the days leading up to November 11, 2005 contributes to an understanding of this extreme precipitation event.

On November 9, 2005 a large cyclone made landfall off the western coast of North America at the Canadian-US border, advecting large amounts of warm, moist air, resulting in high precipitation over the Cascade and Rocky Mountain ranges. On the 10th of November a low pressure system developed in the lee of the northern Rockies and reached its peak strength on the 11th over Robertson Lake station. **Figure 4** shows the daily precipitation field from NCEP/CFSR for November 11, 2005. It depicts precipitation over the areas in the form of snow. **Figure 5** shows the mean field of wind speed at the 250 mb height (jet stream level) from NCEP/CFSR on November 11, 2005. Baroclinic waves migrate from the Pacific coast inland and by the 11th a trough is located over north western Canada. The region

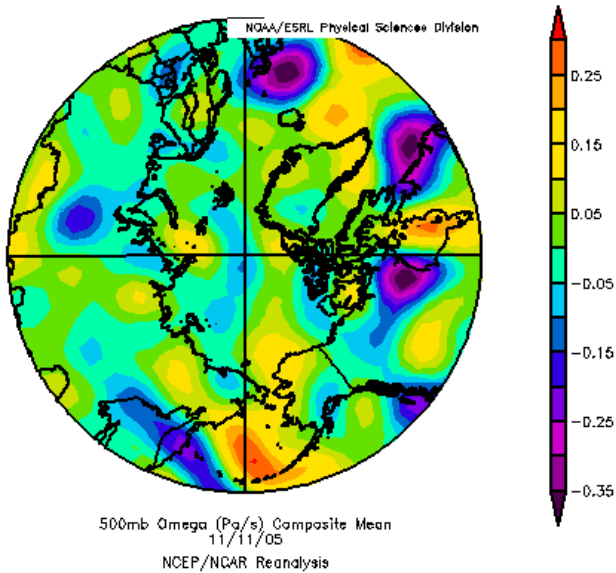


Figure 6: Omega at 500hPa as generated by NCEP/CFSR for the event on 11/11/05

ahead of a trough is the preferred area for cyclogenesis to occur (Serreze and Barry 2014); this corresponds to the location of the low pressure system that drove the extreme event on this day. Strong upper-level divergent winds supported surface level convergence and uplift, which is corroborated by the mean omega field at the 500 hPa level (the approximate level of no-divergence where vertical motion is maximized) generated by NCEP/NCAR in **Figure 6**. Note that upward vertical motion means negative omega. In the vicinity of the gauging station there is strong upward motion of the atmospheric column. As air is displaced upward, surrounding air converges into the region, causing low surface pressure and cyclone deepening. This is consistent with the SLP field shown in figure 4, which depicts a low pressure system situated within the area of vertical motion.

Temperature data from the GHCN database indicates that the average annual temperature for this region is approximately -10 °C, and for the month of November, average temperatures hover around -19 °C. On the day of this extreme event, the average temperature was approximately -4 °C with a maximum of -2 °C. Pointing to strong warm advection, these temperatures fall

in the 99th percentile of daily mean temperature values for the length of the station record. **Figure 8** shows the field from NCEP/CFSR of temperature anomalies during the extreme precipitation event. Relatively high SATs over central North America penetrate deep into Arctic latitudes extending over the vast majority of Northern Canada; the region of exceptionally high SAT corresponds to the location of the gauging station that recorded the event. Turbulent mixing caused by the cyclone may have increased SATs in the region as lower latitude air was advected poleward for several days prior. Areas with negative temperature anomalies are observed poleward of the Canadian mainland including the region of the Canadian Arctic Archipelago. Hence a large temperature gradient existed between the Canadian mainland and the Arctic Ocean, including the islands of the Archipelago, which may have contributed to cyclone deepening. High SATs would have increased the water holding capacity of the overlying atmosphere and, by reducing static stability, also contributed to vertical uplift through condensation and latent heat release. The low pressure system, upward motion, and high SATs ostensibly suggest sufficient conditions to cause an extreme precipitation event, however, this area is dominated by a continental climate and requires a moisture source to generate the large (for this area) amount of precipitation observed on this day. The field of precipitable water at the time of the event is depicted in **Figure 9**. As previously stated, the Arctic climate is relatively arid due to the low air temperatures that dominate the region, limiting the water holding capacity of the atmosphere. Serreze et al. (2012) assessed tropospheric water vapor content using radiosondes and atmospheric reanalysis. They report that the tropospheric water vapor content over the Canadian Arctic Archipelago averages approximately 2.5 mm or

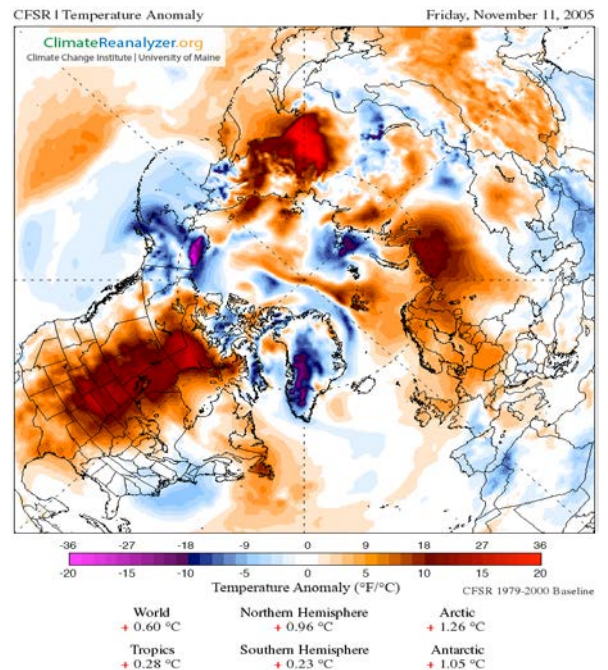


Figure 8: Mean temperature anomaly field for the event on November 11, 2005 generated by NCEP/CFSR

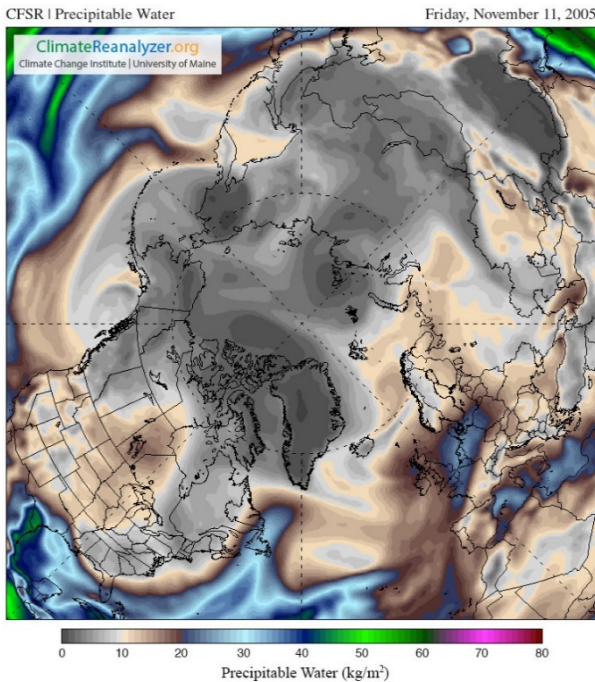


Figure 9: Mean fields of water vapor content from NCEP/CFSR

less during the winter months (Serreze et al. 2012). The available water content of the atmospheric column over northern North America, corresponding with the temperature anomaly field, at the time of the event is approximately 8 mm. The high water vapor content is consistent with the increase in SAT and horizontal vapor flux convergence from the Pacific.

In summary, the formation of an extratropical cyclone on the leeside of the Rocky Mountains and anomalously high SAT over northern North America appear to have driven this extreme event through convergence and frontal uplift. Sharp temperature gradients between the Arctic Ocean and Canadian mainland may have contributed to cyclone deepening over the region. Enhanced mixing may have driven high SAT and increased the water holding capacity of the overlying atmosphere, which supplied the necessary water vapor to generate an extreme precipitation event.

4.2 Qikiqtarjuaq A, Canada

Canadian gauging station Qikiqtarjuaq A is on the southeastern coast of Baffin Island, located on the western side of the Greenland Ice sheet in the Canadian Arctic Archipelago. Baffin Island stretches

across three Arctic Zones, and its landscape is largely dominated by permafrost in all but the southernmost regions (Miller et al. 2005). The entire island sits above treeline and the terrain is predominately mountainous (Fargey et al. 2014). Baffin Island displays some spatial variability regarding annual precipitation and mean temperatures. Annual precipitation averages between 200 and 300 mm over the majority of the island and local winter maxima on the coasts average 500-600 mm. Mean annual temperatures across the island range from -5°C in the south to -15°C in the north (Miller et al. 2005). Qikiqtarjuaq A is situated between the Hall and Meta Incongnita Peninsulas on the southern portion of the island. The selected extreme precipitation event occurred on September 4, 2008 and totaled 50 mm, which falls into the 99.9th percentile of the station’s record. While many precipitation events in the area of Baffin Island are influenced by the Greenland Ice Sheet, the extreme event on this day appears to have been driven by synoptic scale wave patterns, local orography, and anomalous SST. In the days leading up to the extreme event on September 4, 2008 a western trough eastern ridge wave pattern dominated North America. The westerly migration of the mid tropospheric wave placed the diverging arm of the trough in the vicinity of Baffin Island by the fourth of September. **Figure 10** shows the mean wind speed at the 250 mb height from the NCEP/CFSR reanalysis. As noted earlier, the area ahead of a trough favors surface level convergence and upper-level divergence and thus is a preferred area for cyclogenesis (Serreze and Barry 2014). A cold front is advancing from the northwest and is forcing the warm mid-latitude air upwards. This is consistent with the precipitation field

across three Arctic Zones, and its landscape is largely dominated by permafrost in all but the southernmost regions (Miller et al. 2005). The entire island sits above treeline and the terrain is predominately mountainous (Fargey et al. 2014). Baffin Island displays some spatial variability regarding annual precipitation and mean temperatures. Annual precipitation averages between 200 and 300 mm over the majority of the island and local winter maxima on the coasts average 500-600 mm. Mean annual temperatures across the island range from -5°C in the south to -15°C in the north (Miller et al. 2005). Qikiqtarjuaq A is situated between the Hall and Meta Incongnita Peninsulas on the southern portion of the island. The selected extreme precipitation event occurred on September 4, 2008 and totaled 50 mm, which falls into the 99.9th percentile of the station’s record. While many precipitation events in the area of Baffin Island are influenced by the Greenland Ice Sheet, the extreme event on this day appears to have been driven by synoptic scale wave patterns, local orography, and anomalous SST. In the days leading up to the extreme event on September 4, 2008 a western trough eastern ridge wave pattern dominated North America. The westerly migration of the mid tropospheric wave placed the diverging arm of the trough in the vicinity of Baffin Island by the fourth of September. **Figure 10** shows the mean wind speed at the 250 mb height from the NCEP/CFSR reanalysis. As noted earlier, the area ahead of a trough favors surface level convergence and upper-level divergence and thus is a preferred area for cyclogenesis (Serreze and Barry 2014). A cold front is advancing from the northwest and is forcing the warm mid-latitude air upwards. This is consistent with the precipitation field

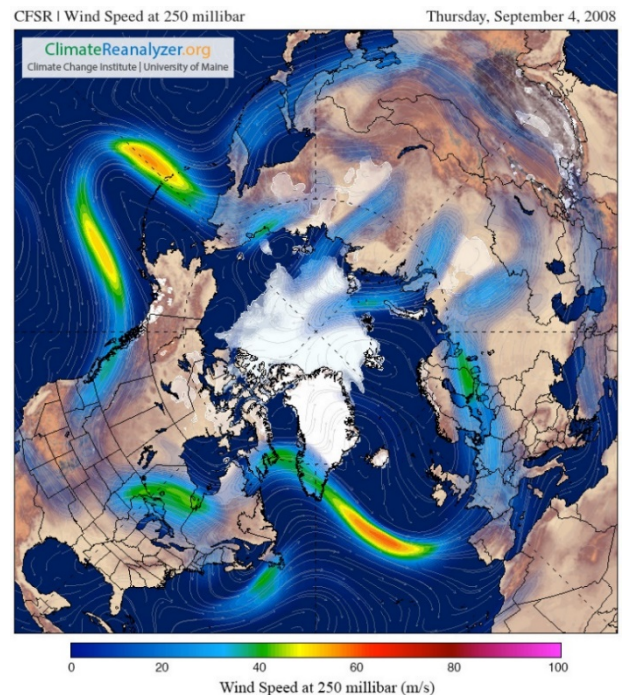


Figure 10: Wind speed at the 250mb height on September 4, 2008 generated from the NCEP/CFSR effort

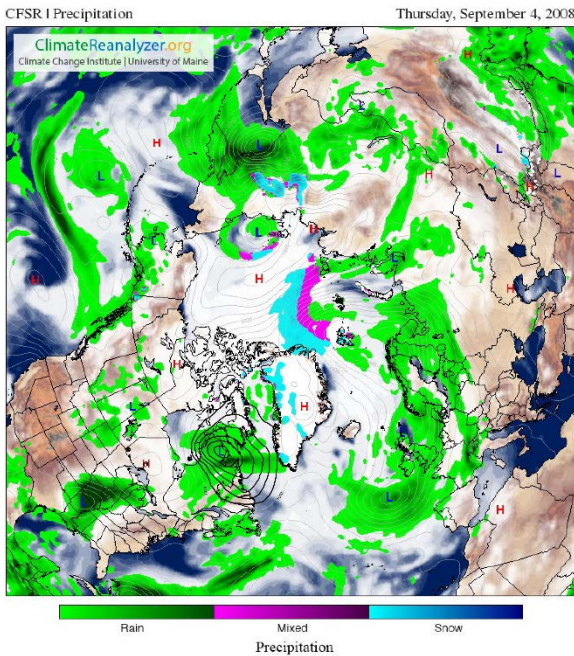


Figure 11: Precipitation field from NCEP/CFSR for September 4, 2008

generated by NCEP/CFSR (Figure 11). A precipitating low pressure system is present in the area that corresponds with the region ahead of the trough. While this cyclone played a significant role in this extreme event, several other factors likely contributed to the observed precipitation extreme.

Sea surface temperatures, in the days prior to and including the extreme event, were anomalously high in Hudson Bay and in the waters of the Davis Strait. Figure 12 shows the mean SST anomaly from NCEP/CFSR for September 4, 2008. Temperature anomalies of up to 2°C are observed in Hudson Bay, Hudson Strait, and the Davis Strait. High SSTs help to increase ET, which in turn increases the water vapor content of the overlying atmosphere. As the cyclone approached Baffin Island, it advected warm southerly air into the region likely allowing more of the water vapor that was evaporated from the sea surface to be stored in the atmosphere. Figure 13 shows the mean precipitable water field from NCEP/CFSR. The atmospheric water content of the overlying column has above average precipitable water resulting from the advection of warm southerly air and, likely, the high SSTs in the area. Serreze et al. (2012) document statistically significant positive trends in water vapor for this region. According to

that study, the atmospheric column just south of Baffin Island is gaining approximately 0.75-1mm of water vapor per decade. These numbers may seem trivial until put in the context of an atmospheric column that typically holds less than 8 mm of water during the autumn (Serreze et al. 2012).

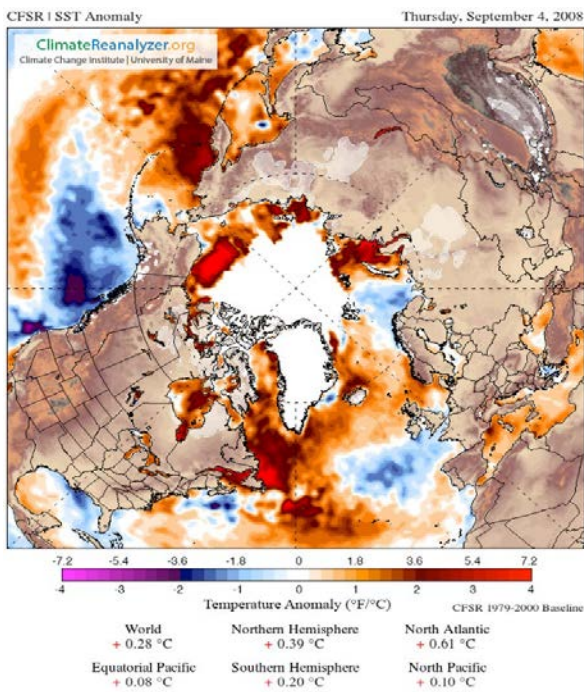


Figure 12: SST anomalies on the day of the event from NCEP/NCAR

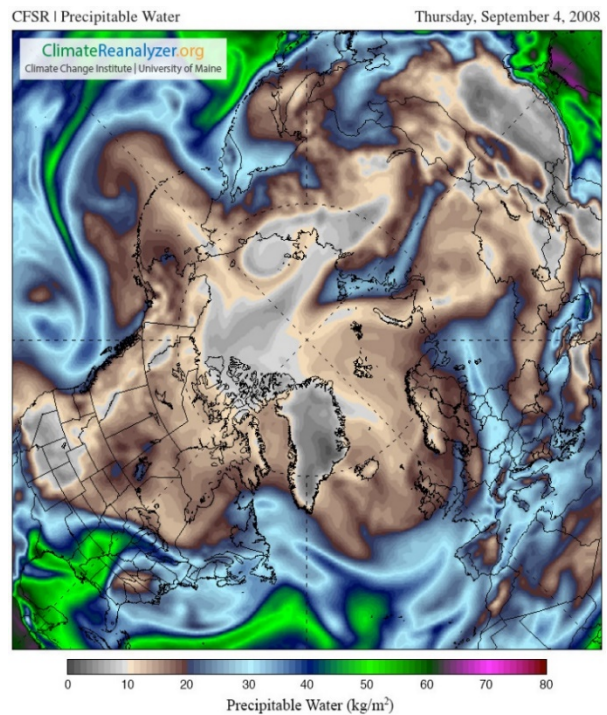


Figure 13: precipitable water on September 4, 2008 as generated from NCEP/CFSR

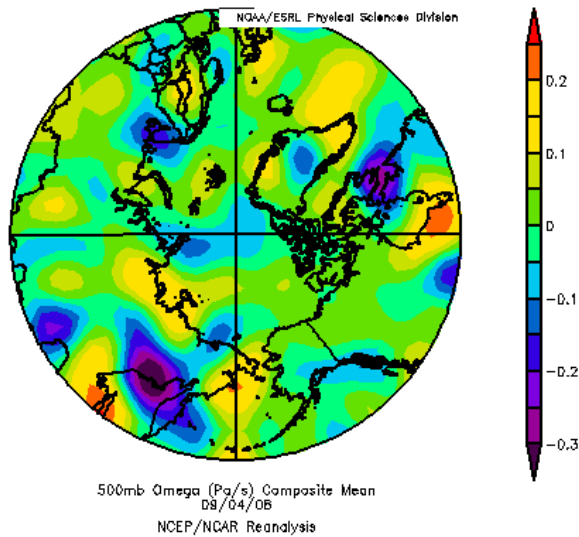


Figure 14: result of NCEP/NCAR reanalysis for composite anomalies of vertical uplift

Uplift of an air mass is required to generate precipitation, and during this event two sources of uplift were likely in play; the advancing cold front and local orography. The Hall Peninsula is home to the Grinnel Ice Cap, which reaches its peak elevation of 1,200m above sea level (Andrews et al. 2002). The mountainous landscape rises abruptly from the surrounding waters causing rapid cooling of air parcels as they lift from the sea surface. Strong vertical uplift generates surface convergence and low SLP which are conducive to heavy precipitation. **Figure 14** shows the mean 500 hPa omega fields from NCEP/NCAR SLP can be seen in Figure 11. Strong vertical uplift in the area of the Hall and Meta Incognita Peninsulas is observed. As a parcel is forced upwards, air converges at the surface, consistent with the low pressure system in the area seen in Figure 11.

In summary, the region of the Canadian Arctic Archipelago that contains Baffin Island is limited in precipitation primarily as a result of low air temperatures, however, anomalously high SST and SAT were present which significantly increased the water vapor content of the overlying atmosphere and supplied the

conditions necessary to generate an extreme precipitation event. Glisan and Gutowski (2014) documented the significant contribution of orography to the enhancement of extreme precipitation in eastern Canada. They found that extreme events in Canada east tend to occur in areas with high topographic features, particularly in areas where low level moisture flux converged from adjacent ocean bodies (Glisan and Gutowski 2014). The tendency for extremes to occur over mountainous areas suggests a significant orographic contribution to extreme precipitation in this region.

4.3 Kelly Station, Alaska

Kelly station is located in Alaska above the Seward Peninsula. The station is close to the northeastern Alaskan coast and the general climate surrounding the gauging station is classified as maritime polar although mean winter temperatures are much lower than other maritime polar climates due to the presence of sea ice (Serreze and Barry 2014). The region is dominated by marshy inlets and annual precipitation averages less than 250mm (Wendler et al. 2010). Over the past several decades the Arctic has been exhibiting profound climatic changes with some of the most pronounced temperature changes occurring in Northern Alaska (Shulski and Wendler 2007). On July 23, 2011 the gauging station measured 34 mm of precipitation in a 24-hour period. This event lies in the 99.9th percentile of the station’s record. For many land areas in the Arctic, precipitation is at a maximum in the summer, when convective storms become fairly common (Serreze and Barry 2014). Regionally, the Arctic frontal zone [Serreze et al., 2001] contributes to summer precipitation maxima. Areas where the Arctic frontal zone is most prevalent, such as Alaska, Eurasia, and western Canada, are also preferred areas for cyclone deepening (Crawford and Serreze, in revision). In some areas, up to 60% of annual precipitation

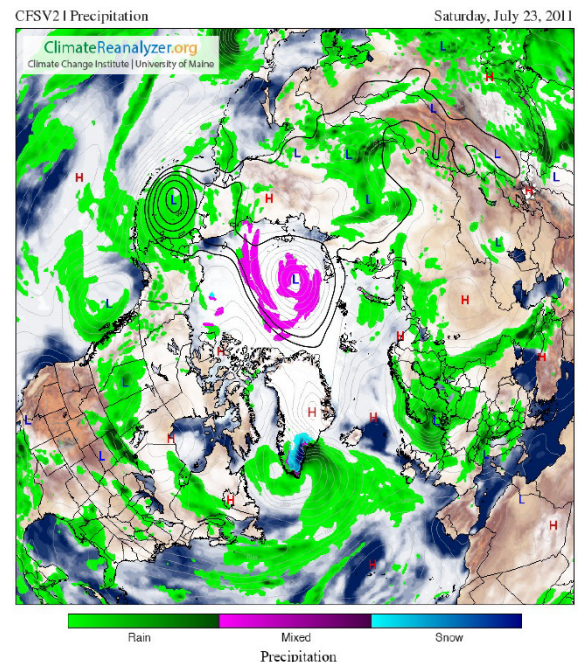


Figure 15: Mean precipitation and SLP fields generated by NCEP/CFSR

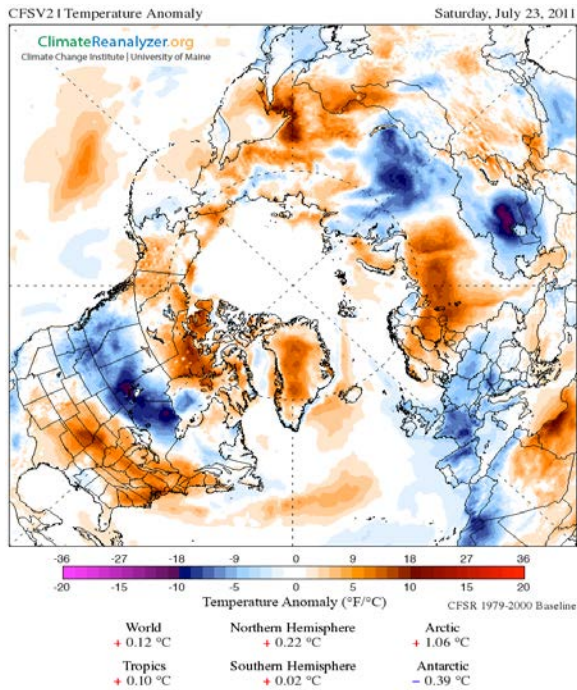


Figure 16: SAT anomaly fields from NCEP/NCAR

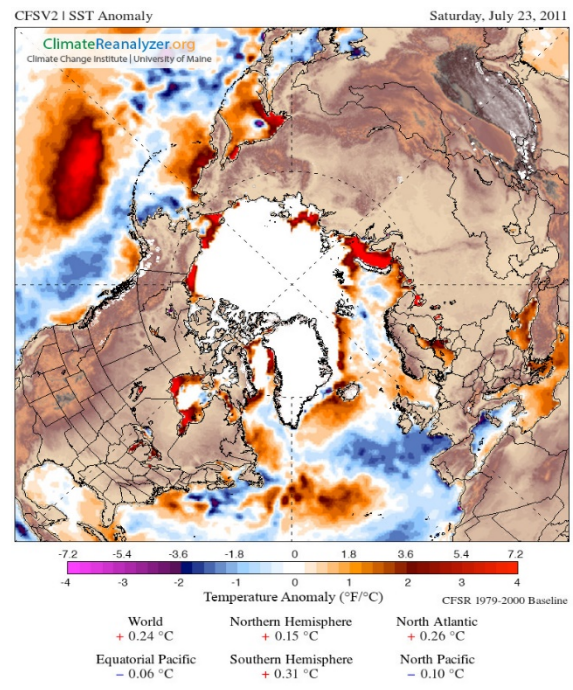


Figure 17: SST anomaly fields NCEP/NCAR

falls during summer, and the summer frontal zone appears to be a strong contributor. In Alaska, typically 50% of annual precipitation falls in summer (Lynch et al. 2001; Serreze and Barry 2014). In addition to the influence of the Arctic frontal zone, the climate regime of the northwestern coast is influenced by the Aleutian low, proximity to the Chukchi Sea, strong winds, orography, and temperature, all of which contributed to the extreme event under investigation.

The mean SLP and mean precipitation on the day of the extreme event are shown in **Figure 15**. Note the deep low west of Alaska, which is located downstream of a mid-tropospheric trough where upper-level divergence creates favorable conditions for cyclone development (Serreze and Barry 2014). The position of the low favored the advection of moist air into the vicinity of Kelly Station. On July 23, 2011 a large temperature gradient existed between land and ocean. **Figure 16** shows the SAT anomaly field and **Figure 17** shows the SST anomaly field at the time of the event. A slightly negative temperature anomaly can be observed over the Chukchi Sea while a positive anomaly is observed over Alaska. As previously discussed, sharp temperature gradients, provided that they extend through a sufficiently deep layer of the atmosphere, favor cyclone deepening. Inflow of cold sea air over the heated land surface would have also intensified uplift during the event (Matveeva et al. 2015) as would local orography. Glisan and Gutowski (2014) found that strong vertical motion combined with low level moisture flux convergence were common factors in extreme events analyzed over the region. The precipitation fields for this event strongly coincide with the temperature anomaly and wind fields.

Figure 18 depicts the wind velocities observed on the day of the extreme event. The wind pattern suggests that as air approached the coast line, local orography forced the air mass upward as the topographic relief increased towards the tail end of the Brooks Range.

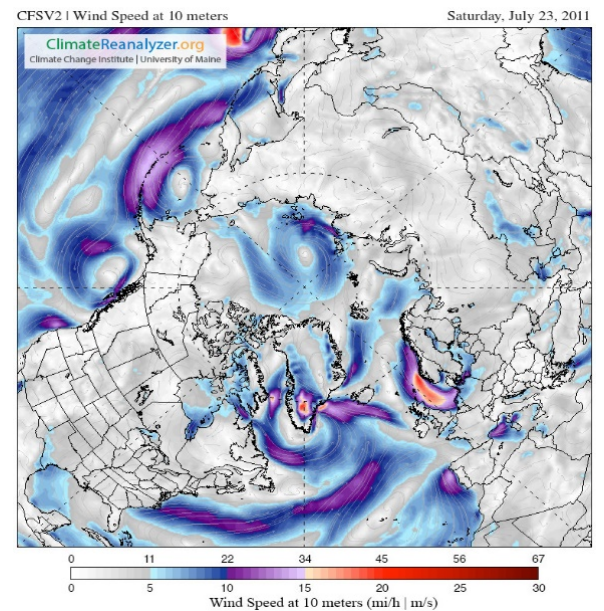


Figure 18: Wind speed at 10 meters as depicted by NCEP/CFSR for July 23, 2011

According to historical records from *Weather Underground* (2011), the dew point on July 23, 2011 was 55°F which is very high for the area. High dew points are conducive to precipitation and the lifted air parcel would not have had to cool much before condensation occurs. In summary, the combination of a mid-tropospheric trough, differential heating, strong winds, orography, and the advection of moisture towards the land surface created favorable conditions for precipitation at Kelly Station.

5.0 Trends Analysis Results

| Frequency | Annual | Seasonal | Monthly |
|--------------------|------------|--|---|
| Circumpolar | No Changes | Increasing Spring Decreasing Summer | Increase: March, April, May, October Decrease: July, August |
| Region 1 | No Changes | Increasing Winter Decreasing Summer | Increasing November Decreasing August |
| Region 2 | No Changes | No Changes | No Changes |
| Region 3 | No Changes | Increasing Spring Decreasing Winter | Decrease: December, January, February, August |
| Region 4 | No Changes | No Changes | Decrease: December, January, February, August |

| Intensity | Annual | Seasonal | Monthly |
|--------------------|------------|--|--|
| Circumpolar | Increase | Increase Spring Decrease: Winter, Summer, Fall | Increase: March, April, May, June, October Decrease August |
| Region 1 | Increase | Increase: All Seasons | Increase: All Months |
| Region 2 | No Changes | No Changes | No Changes |
| Region 3 | Decrease | Decrease: All Seasons | Increase: Jan, Feb, March, July, Aug, Sept, Oct, Nov, Dec |
| Region 4 | Decrease | Decrease: All Seasons | Decrease: January, July, August, December |

Table 2: Table summarizing the results of frequency analysis on circumpolar and regional zones on various timescales

Table 2: Table summarizing the results of intensity analysis on circumpolar and regional zones on various time scales

For a given month, the number of times an individual station recorded an event that was greater than or equal to its threshold value was summed and recorded in a frequency table. Similarly, the millimeter value of all extreme events was summed into a single intensity value for that month and station. Using the frequency and intensity table, data could be subset based on time and location. However, there was a large bias in the number of precipitation reports between the years of 1990 and 2000. This decade had approximately three times as many valid (non-missing) reports as other decades and not all stations were actively recording in all months. The imbalance required that the frequency and intensity table be normalized to the number of active stations recording for a given time period. Using time as the independent variable and frequency (intensity) as the dependent variable, non-parametric correlation tests were conducted on annual, seasonal, and monthly timescales for the Arctic as a whole, and then for each of the four regions.

The aggregated results of analyses are included in **Table 2**. Frequency and intensity trends show a large degree of spatial and temporal variability. On large spatial scales (i.e., the entire Arctic) the frequency of extreme precipitation events shows no changes on annual time scales. However, statistically significant changes are observed on seasonal and monthly timescales. On a seasonal timescale, the frequency of extreme precipitation events appears to be increasing during the spring and decreasing during the summer months. Similarly, intensity appears to be increasing both on an annual timescale and seasonal/monthly timescales, however, the intensity trends for the Arctic as a whole are largely driven by an anomalous spike in the Region 1 precipitation from 2004-2006.

On smaller spatial scales, variability in the frequency and intensity of extreme precipitation is greater. Region 1, which includes Canada, the Canadian Arctic Archipelago, and Alaska, also shows no change in extreme precipitation on annual timescales. However, on seasonal and monthly timescales both positive and negative trends are present. The

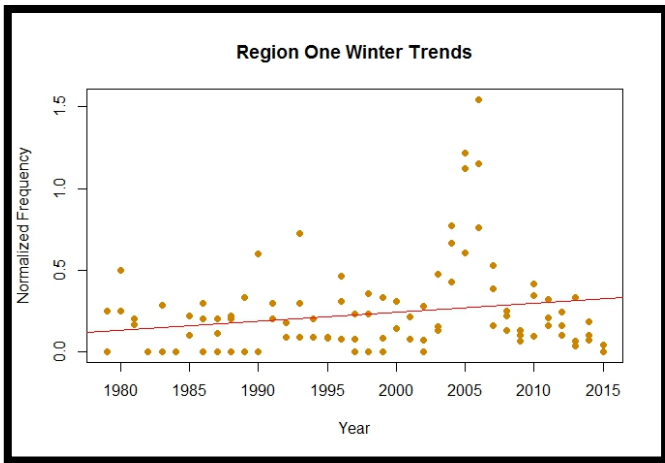


Figure 19: Region One's trend in extreme precipitation for the winter months based on a normalized frequency

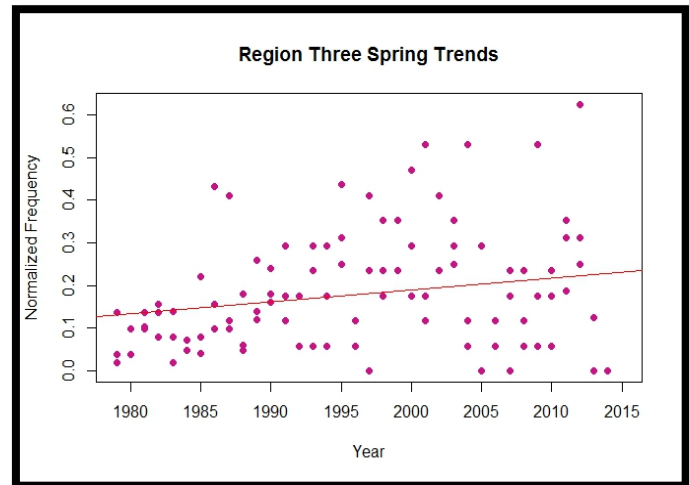


Figure 21: Increasing frequency of extreme precipitation events observed for Region Three based on a normalized frequency

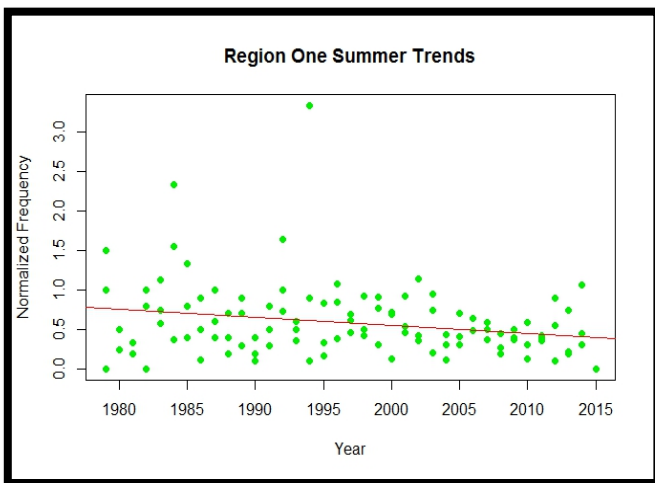


Figure 20: Decreasing frequency of extreme precipitation for Region One during the summer, based on normalized frequency

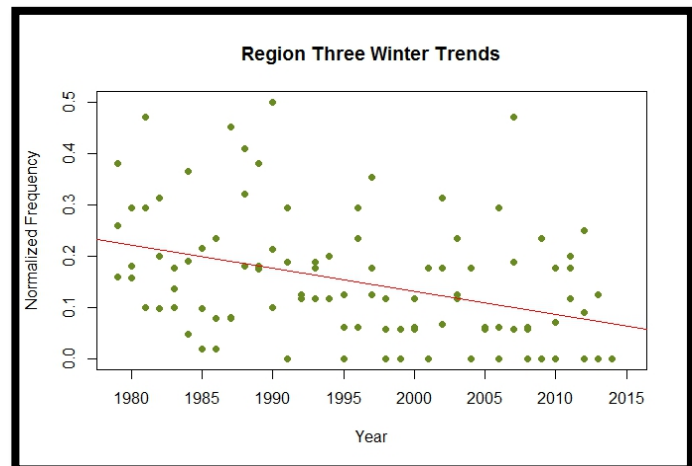


Figure 22: Observed decreases in the frequency of extreme precipitation events for Region Three based off of a normalized frequency

frequency of extreme events seems to be increasing in the winter, specifically in November. Conversely, negative trends appear in the summer, specifically during August. **Figures 19 and 20** outline the results of the correlation test for this region, and highlight the dramatic increase in precipitation between the years 2004 and 2006 (Figure 20). The intensity of extreme precipitation events in Region 1 appear to be increasing in all seasons and months, however, it is likely that the aforementioned years have a significant impact on these results. Possible reasons for this spike in precipitation will be addressed shortly.

Region 2, which contains the area influenced by the North Atlantic storm track, shows no significant changes on any timescale. By contrast, Region 3, which encompasses northwest Siberia, shows significant trends on seasonal timescales, including an increasing frequency of extreme precipitation in the spring (**Figure 21**) and decreasing frequency in the winter (**Figure 22**), and trends in intensity are negative on all timescales. Region 4 displays a decreasing frequency of extreme events on monthly timescales, largely centered on the winter months, however, the intensity of extreme events appears to be decreasing across all timescales.

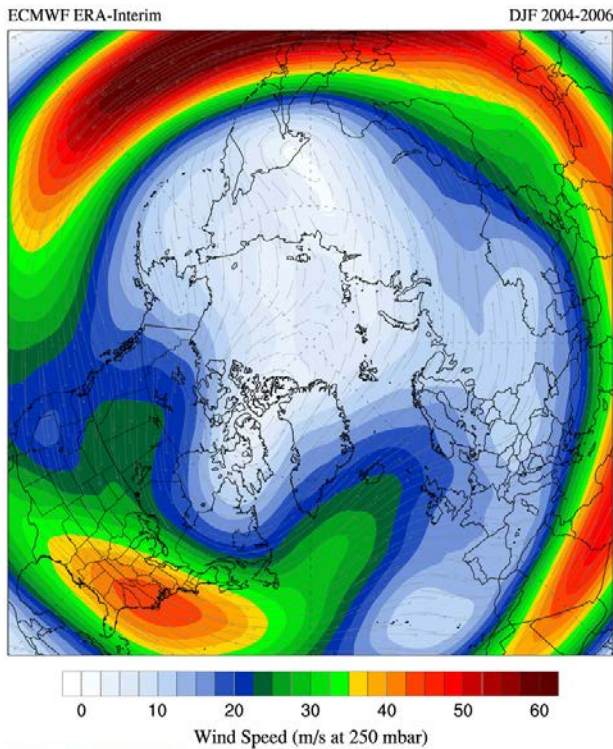


Figure 23: Wind speed at the 250 hPa height for the winter of 2004-2006 generated by NCEP/CFSR

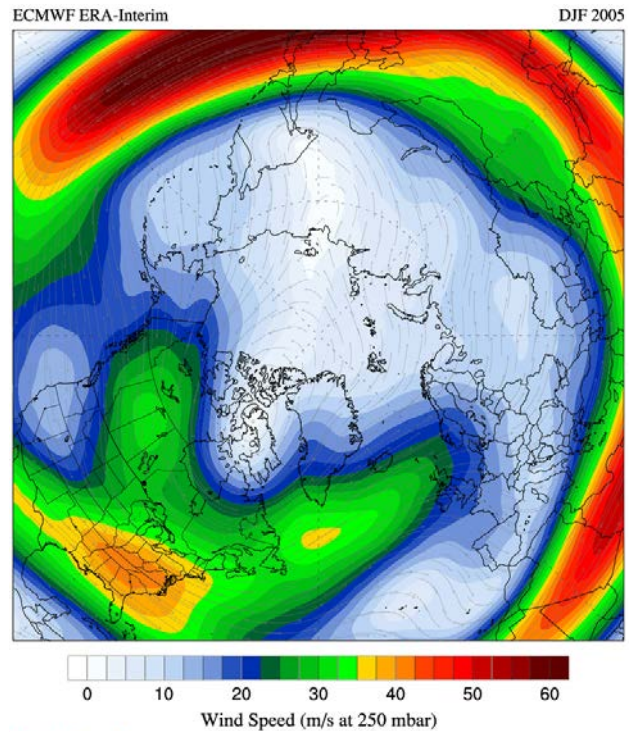


Figure 24: Wind speed at the 250 hPa height for winter 2005 generated by NCEP/CFSR

6.0 Discussion

The results presented above are broadly consistent with those from other recent research, which has shown large spatiotemporal variability in hydrologic changes taking place within the Arctic. Unsurprisingly, the most pronounced changes observed from this study are taking place in Region 1 - the area encompassing the Canadian Arctic Archipelago, Canadian mainland territory, and Alaska.

Correlation tests for Region 1 reveal that extreme precipitation events, for the region as a whole, are increasing during the winter months and decreasing during the summer months. Spatial variability in topography and the distribution of water sources within the region require that data be subset to determine where within Region 1 these changes are occurring. Stations were grouped into three neighborhoods 1) the Canadian Arctic Archipelago 2) central Canada and 3) Alaska. Station records within these neighborhoods were then analyzed to determine which local neighborhood(s) were driving the observed changes in the region.

The analysis reveals that centrally located stations within Region 1 are generally not experiencing significant trends in any season, which suggests that the winter increase in extreme precipitation, for the region as a whole, is being driven by the coastal stations in the CAA and Alaska. This is consistent with research focused on trends in water vapor content; the CAA and Alaska are areas associated with significant positive increases in water vapor, whereas central Canada has experienced smaller increases. Figure 20 highlights the spike in extreme precipitation frequency during winter. Further inspection of the data reveal that both the Alaskan and CAA stations saw a number of extreme events in these years, associated with positive SAT anomalies and low sea ice extent, however, the anomalous spike in winter extreme precipitation between 2004-2006 is primarily reflected in the CAA station records. The winter spike may be associated with declining sea ice, increased energy content, and sudden stratospheric warming events.

Simmonds and Keay (2009) suggest that the observed decline in sea ice extent increases the available energy for cyclonic systems, which would manifest itself as enhanced development of preexisting cyclones. Sharp reductions in sea ice extent during the summer months directly influence circulation patterns in late autumn and winter. Heat energy that is gained by the ocean during the summer is released during the autumn and can have significant impact on tropospheric temperatures (Overland and Wang, 2010) and atmospheric stability. The year 2005 (the peak in winter extreme precipitation frequency for Region 1) marked the beginning of steep reductions in sea ice extent, particularly in the areas of the Barents/Kara Seas and Baffin Bay (Simmonds and Keay 2009; Park et al. 2015) which may have influenced the trends, or lack thereof, observed in Regions 1 and 2. Simmonds and Keay (2009) found a statistically significant correlation between low sea ice extent and stronger/larger cyclones. They also note that September synoptic activity has also been variable; even minor changes in synoptic activity may lead to enhanced horizontal sensible heat and moisture transport into the Arctic, leading to anomalous SATs and a greater potential for greater cyclone deepening, which is consistent with the results of this study. While Simmonds and Keay (2009) found no evidence of increasing cyclone activity, they did find increases in cyclone deepening over the Canadian Arctic potentially due to enhanced energy availability in the region.

Winter circulation in the Arctic is characterized by an asymmetrical winter vortex with large troughs over eastern North America and western Asia and ridges over western North America, eastern Atlantic and central Asia (Serreze and Barry, 2014). Winds at the jet stream level (250 hPa) during the winters of 2004-2006 from NCEP/CFSR (**Figure 23**) deviate somewhat from the general circulation pattern described previously. **Figure 24** shows composite winter circulation at the 250 hPa for just 2005 from NCEP/CFSR. Both figures show changes in the winter vortex and in the placement of the eastern North American trough compared to climatology. The diverging arm of the eastern North American trough corresponds to the general location of the North Atlantic storm track, which typically runs east of the Greenland Ice sheet. Figures 24 and 25 show a westward shift in the eastern North American trough where the diverging arm is intersected by the Greenland Ice sheet (Figure 24) or completely shifted to the western side of the ice sheet (Figure 25). Enhanced penetration of southerly air into the Arctic may have shifted the placement of the eastern North American trough and increased the rate of upper-level divergence and surface level convergence, which would have created favorable conditions for cyclone formation and precipitation. The circulation during the winter of 2005 (the peak of the anomalous spike) shows a pronounced trough over the CAA, which would have favored cyclone formation in this area. Local orography may have contributed to the occurrence of extreme events via the rapid uplift of air as it converged into an area experiencing prolonged SAT anomalies and increased water vapor content. There is little indication that these events signal the involvement of the AO as the index during this time period was generally negative.

Sudden stratospheric warming may have also contributed to the 2004-2006 extreme precipitation spike. Peters et al. (2010) investigated the sudden stratospheric warming event that split the polar vortex in the winter of 2003 and found that the following winters (2004-2005) experienced ozone depletion of 116 +/- 10 Dobson Units and was accompanied by very cold lower stratospheric air temperatures and enhanced westerly zonal wind speeds. Positive mean zonal tropospheric winds allow for the vertical propagation of waves into the stratosphere, which may have enhanced upper-level divergence during this time period. Ozone depletion beginning in 2002 may have also inhibited planetary waves propagating towards the polar vortex which may have decreased variations in wave activity in the troposphere prolonging the lifetime of the eastern North American trough seen in Figure 24 (Peters et al. 2010).

While summer extreme precipitation event for Region 1 as a whole appear to be decreasing, on the Pacific side of Region 1, Alaskan stations not only exhibit increases in the frequency of winter extreme precipitation, but also show increases in the frequency of summer extreme precipitation which is broadly consistent with current research (McCabe et al. 2001; Zhang et al. 2004; Serreze and Barrett 2008). Positive trends in water vapor have been found over Alaska for both winter and summer. Winter increases in the Pacific sector may be attributed to anomalous spikes in SAT over land

areas in combination with increased water vapor content. Summer increases over Alaska may be associated with increasing frontal frequencies resulting from enhanced surface heating and decreasing mean SLP over the CAO, which may strengthen the 500 hPa polar vortex and increase mass transfers from lower latitudes into the Arctic (Serreze and Barrett, 2008). Serreze et al. (2012) found that significant positive water vapor anomalies in this area during the summer were closely co-located with negative sea ice anomalies which were also in the area.

The lack of significant trends in Region 2 is perhaps surprising as this region has been linked to some of the most dramatic increases in water vapor content over the past several decades (Serreze et al. 2012) and is quite sensitive to reduced sea ice extent and SST variability. The lack of significant results may be attributed to uncertainty within the data record, limited station record availability for the region, or perhaps a poleward shift in the location of the North Atlantic storm track. The IPCC AR5 suggest that a poleward shift since the 1970's is *likely*, however, there remains significant debate on this topic and a shift has yet to be convincingly demonstrated.

Region 3, which encompasses northwest Siberia, has experienced negative trends in the frequency of extreme precipitation during the winter months and positive trends in the spring. This is consistent with recent research (Serreze and Barrett 2008). McCabe et al. (2001) found that the largest seasonal decreases in SLP over the CAO are associated with the seasons experiencing the most warming; winter and spring. The Siberian high dominates Eurasia during the winter season and a poleward shift in the location of the attendant ridge could contribute to the decrease in extreme precipitation. A strong Siberian high is associated with very low air temperatures, which decreases the water holding capacity of the atmosphere, as such decreased water vapor content has also been observed in the region (Serreze et al. 2012). Similarly, the transition to spring decreases the strength of the Siberian High as the center of the 500hPa polar vortex migrates over the CAO (Serreze and Barrett 2008). Increased warming in the shoulder seasons and reductions in sea ice extent may result in the Urals trough migrating eastward earlier in the year (i.e the spring) which is associated with the enhancement of the Arctic Frontal Zone and increased precipitation. Region 4 displays similar trends in winter extreme precipitation as Region 3 and is largely dominated by the same atmospheric circulation patterns.

7.0 Conclusion

Spatiotemporal patterns of extreme precipitation in the Arctic have varied over the past several decades. These variations display significant spatial and temporal heterogeneity with some areas of the Arctic seeing an increasing frequency of extreme precipitation and others have negative trends. Increasing frequency of extreme events appears to be driven by anomalously high air and sea surface temperatures and increases in atmospheric water vapor content. This study suggests that the observed changes in extreme events within Regions 3 and 4 are not strongly related to atmospheric variability whereas in Region 1 atmospheric variability seems to play a significant role.

This study serves to shed some light on a largely under-researched area of the Arctic climate system and is by no means conclusive. Data biases and uncertainty likely affect the results of this study and need to be further addressed. This study was unable to investigate changes in extreme precipitation frequency over the Arctic Ocean as there is no monitoring program in this critical area. Further, investigation into precipitation phase during these events would also be beneficial as rain on snow events can have pronounced environmental impacts.

8.0 References

- Alexander, M. A., Bhatt, U. S., Walsh, J. E., Timlin, M. S., Miller, J. S., & Scott, J. D. (2004). The atmospheric response to realistic arctic sea ice anomalies in an AGCM during winter. *Journal of Climate*, *17*(5), 890–905. doi: [http://dx.doi.org/10.1175/1520-0442\(2004\)017<0890:TARTRA>2.0.CO;2](http://dx.doi.org/10.1175/1520-0442(2004)017<0890:TARTRA>2.0.CO;2)
- Andrews, J. T., Holdsworth G., & Jacobs J. D. (2002). Glaciers of North America-Glaciers of Canada Glaciers of the Arctic Islands Glaciers of Baffin Island. In R. S. Williams Jr. & J. G. Ferrigno (Eds.), *Satellite image atlas of glaciers of the world - North America: United States geological survey professional paper 1386-J* (pp. J165-J198). Washington, DC: United States Government Printing Office. Retrieved from <http://pubs.usgs.gov/pp/p1386j/baffinisland/baffinlores.pdf>.
- Bhatt, U. S., Alexander, M. A., Deser, C., Walsh, J. E., Miller, J. S., Timlin, M. S., . . . Tomas, R. A. (2008). The atmospheric response to realistic reduced summer arctic sea ice anomalies. In E. T. DeWeaver, C. M. Bitz & L.B. Tremblay (Eds.) *Geophysical monograph series, vol. 180, Arctic sea ice decline: Observations, projections, mechanisms, and implications* (pp. 91-110). Washington, DC: American Geophysical Union. doi: 10.1029/180GM08
- Center for International Earth Science Information Network - CIESIN - Columbia University (2012). National Aggregates of Geospatial Data Collection: Population, Landscape, And Climate Estimates, Version 3 (PLACE III). Palisades, NY: NASA Socioeconomic Data and Applications Center (SEDAC). Retrieved from http://sedac.ciesin.columbia.edu/es/papers/Coastal_Zone_Pop_Method.pdf
- Cohen, J. & Barlow, M. (2005). The NAO, the AO, and Global Warming: How Closely Related? *Journal of Climate*, *18*(21), 4498–4513. doi: <http://dx.doi.org/10.1175/JCLI3530.1>
- Crawford, A.D. & Serreze, M. C. (in revision). Does the Arctic Frontal Zone impact summer cyclone activity in the Arctic Ocean? *Journal of Climate*.
- Cvijanovic, I., Caldeira, K., & MacMartin, D. G. (2015). Impacts of ocean albedo alteration on Arctic sea ice restoration and Northern Hemisphere climate. *Environmental Research Letters*, *10*(4). doi: 10.1088/1748-9326/10/4/044020
- Dee, D. P., Uppala, S. M., Simmons, A. J., Berrisford, P., Poli, P., Kobayashi, S., . . . Vitart, F. (2011). The ERA-Interim reanalysis: Configuration and performance of the data assimilation system. *Quarterly Journal of the Royal Meteorological Society*, *137*(656), 553-597. doi: 10.1002/qj.828
- Deser, C., Tomas, R. A., & Peng, S. (2007). The transient atmospheric circulation response to North Atlantic SST and sea ice anomalies. *Journal of Climate*, *20*(18),4751–67. doi:10.1175/JCLI4278.1.
- Devlin, J. E. & Finkelstein, S.A. (2011). Local physiographic controls on the responses of Arctic lakes to climate warming in Sirmilik National Park, Nunavut, Canada. *Journal of Paleolimnology*, *45*(1), 23-39. doi: 10.1007/s10933-010-9477-6.
- Fargey, S., Hanesiak, J., Stewart, R., & Wolde, M. (2014). Aircraft observations of orographic cloud and precipitation features over southern Baffin Island, Nunavut, Canada. *Atmosphere-Ocean*, *52*(1), 54–76. doi:10.1080/07055900.2013.855624.
- Francis, J. A. & Hunter, E. (2007). Drivers of declining sea ice in the Arctic winter. *Geophysical Research Letters*, *34*, L17503. doi:10.1029/2007GL030995

- Francis, J. A. & Vavrus, S. J. (2012). Evidence linking Arctic amplification to extreme weather in mid-latitudes. *Geophysical Research Letters*, 39(6), L06801. doi:10.1029/2012GL051000.
- Francis, J. A., Chan, W., Leathers, D. J., Miller, J. R., & Veron, D. E. (2009). Winter Northern Hemisphere weather patterns remember summer Arctic sea-ice extent. *Geophysical Research Letters*, 36(7), L07503. doi:10.1029/2009GL037274.
- Glisan, J M. & Gutowski, W. J. (2014). WRF summer extreme daily precipitation over the CORDEX Arctic. *Journal of Geophysical Research Atmospheres*, 119(4), 1720-1732. doi: 10.1002/2013JD020697
- Gong, D. Y. & Ho, C. H. (2002). The Siberian High and climate change over middle to high latitude Asia. *Theoretical and Applied Climatology*, 72(1), 1-9. doi:10.1007/s007040200008.
- Gusakova, M. A. & Karlin, L. N. (2014). Assessment of contribution of greenhouse gases, water vapor, and cloudiness to the variations of global surface air temperature. *Russian Meteorology and Hydrology*, 39(3), 146-151. doi: 10.3103/S1068373914030029
- Hanesiak, J., Stewart, R., Barber, D., Liu, G., Gilligan, J., Desjardins, D., . . . Laplante, A. (2010). Storm studies in the Arctic (STAR). *Bulletin of the American Meteorological Society*, 91(1), 47-68. doi: <http://dx.doi.org/10.1175/2009BAMS2693.1>
- Held, I. M. & Soden, B. J. (2000). Water vapor feedback and global warming. *Annual Review of Energy and the Environment*, 25, 441-475. doi:10.1146/annurev.energy.25.1.441.
- Herman, G. T. & Johnson, W. T. (1978). The sensitivity of the general circulation of Arctic sea ice boundaries: A numerical experiment. *Monthly Weather Review*, 106, 1649-1664. doi: [http://dx.doi.org/10.1175/1520-0493\(1978\)106<1649:TSOTGC>2.0.CO;2](http://dx.doi.org/10.1175/1520-0493(1978)106<1649:TSOTGC>2.0.CO;2)
- Honda, M., Yamazaki, K., Tachibana, Y., & Takeuchi, K. (1996). Influence of Okhotsk sea-ice extent on the atmospheric circulation. *Geophysical Research Letters*, 23, 3595-3598. doi: 10.1029/96GL03474
- Hori, M. E., Inoue, J., Kikuchi, T., Honda, M., & Tachibana, Y. (2011). Recurrence of intraseasonal cold air outbreak during the 2009/2010 winter in Japan and its ties to the atmospheric condition over the Barents-Kara Sea. *SOLA*, 7, 25-28. doi: <http://doi.org/10.2151/sola.2011-007>
- IPCC (2013). *Climate change 2013: The physical science basis. Contribution of working group I to the fifth assessment report of the intergovernmental panel on climate change*. T. F. Stocker, D. Qin, G.-K. Plattner, M. Tignor, S.K. Allen, J. Boschung, A. Nauels, Y. Xia, V. Bex & P.M. Midgley (Eds.). Cambridge, UK & New York, NY: Cambridge University Press. doi:10.1017/CBO9781107415324
- Kalnay, E., Kanamitsu, M., Kistler, R., Collins, W., Deaven, D., Gandin, L., . . . Joseph, D. (1996). The NCEP/NCAR 40-year reanalysis project. *Bulletin of the American Meteorological Society*, 77(3), 437-471. doi: [http://dx.doi.org/10.1175/1520-0477\(1996\)077<0437:TNYRP>2.0.CO;2](http://dx.doi.org/10.1175/1520-0477(1996)077<0437:TNYRP>2.0.CO;2)
- Langen, P. L., & Alexeev, V. A. (2004). Multiple equilibria and asymmetric climates in the CCM3 coupled to an oceanic mixed layer with thermodynamic sea ice. *Geophysical Research Letters*, 31(4), L04201. doi: 10.1029/2003GL019039
- Ludlum, D. M. (1998). *National Audubon Society field guide to North American weather*. New York, NY: Knopf.

- Lynch, A. H., Slater, A. G., & Serreze, M. (2001). The Alaskan Arctic Frontal Zone: Forcing by orography, coastal contrast, and the boreal forest. *Journal of Climate*, *14*(23), 4351-4362. doi: [http://dx.doi.org/10.1175/1520-0442\(2001\)014<4351:TAAFZF>2.0.CO;2](http://dx.doi.org/10.1175/1520-0442(2001)014<4351:TAAFZF>2.0.CO;2)
- Macdonald, R. W., Harner, T., & Fyfe, J. (2005) Recent climate change in the Arctic and its impact on contaminant pathways and interpretation of temporal trend data. *Science of the Total Environment*, *342*(1-3), 5-86. doi: 10.1016/j.scitotenv.2004.12.059
- Magnusdottir, G., Deser, C., & Saravanan, R. (2004). The effects of North Atlantic SST and sea ice anomalies on the winter circulation in CCM3. Part I: Main features and storm track characteristics of the response. *Journal of Climate*, *17*(5), 857-876. doi: [http://dx.doi.org/10.1175/1520-0442\(2004\)017<0857:TEONAS>2.0.CO;2](http://dx.doi.org/10.1175/1520-0442(2004)017<0857:TEONAS>2.0.CO;2)
- Mantua, N. J., Hare, S. R., Zhang, Y., Wallace, J. M., & Francis, R. C. (1997). A Pacific interdecadal climate oscillation with impacts on salmon production. *Bulletin of the American Meteorological Society*, *78*(6), 1069-1079. doi:10.1175/1520-0477(1997)078<1069:APICOW>2.0.CO;2
- Matveeva, T. A., Gushchina, D. Y., & Zolina, O. G. (2015). Large-scale indicators of extreme precipitation in coastal natural-economic zones of the European part of Russia. *Russian Meteorology and Hydrology*, *40*(11), 722-730. doi: 10.3103/S1068373915110023
- McCabe, G. J., Clark, M. P., & Serreze, M. C. (2001). Trends in northern hemisphere surface cyclone frequency and intensity. *Journal of Climate*, *14*(12), 2763-2768. doi:10.1175/1520-0442(2001)014<2763:TINHSC>2.0.CO;2
- McGuire, A. D., Chapin, F. S., III, Walsh, J. E., & Wirth, C. (2006). Integrated regional changes in Arctic climate feedbacks: Implications for the global climate system. *Annual Review of Environment and Resources*, *31*(1), 61-91. doi: 10.1146/annurev.energy.31.020105.100253
- Menne, M.J., I. Durre, B. Korzeniewski, S. McNeal, K. Thomas, X. Yin, S. Anthony, R. Ray, R.S. Vose, B.E. Gleason, & T.G. Houston. (2012). *Global Historical Climatology Network - Daily (GHCN-Daily), Version 3.22 NOAA* [Data file]. National Climatic Data Center. doi: <http://doi.org/10.7289/V5D21VHZ>
- Miller, G. H., Wolfe, A. P., Briner, J. P., Sauer, P. E., & Nesje, A. (2005). Holocene glaciation and climate evolution of Baffin Island, Arctic Canada. *Quaternary Science Reviews*, *24*(14-15), 1703-1721. doi: 10.1016/j.quascirev.2004.06.021
- Mori, M., Watanabe, M., Shiogama, H., Inoue, J., & Kimoto, M. (2014). Robust Arctic sea-ice influence on the frequent Eurasian cold winters in past decades. *Nature Geoscience*, *7*, 869-873. doi: 10.1038/ngeo2277
- Murray, R. J. & Simmonds, I. (1995), Responses of climate and cyclones to reductions in Arctic winter sea ice. *Journal of Geophysical Research*, *100*(C3), 4791-4806. doi:10.1029/94JC02206
- Nakamura, H., Izumi, T., & Sampe, T. (2002). Interannual and decadal modulations recently observed in the Pacific storm track activity and east Asian winter monsoon. *Journal of Climate*, *15*(14), 1855-1874. doi: 10.1175/1520-0442(2002)015<1855:IADMRO>2.0.CO;2
- National Snow and Ice Data Center, compiler. (2006). *Monthly mean precipitation sums at Russian arctic stations, 1966-1990* [Data file]. Boulder, Colorado USA: National Snow and Ice Data Center. doi: <http://dx.doi.org/10.7265/N55H7D6Q>

- Overland, J., Francis, J. A., Hall, R., Hanna, E., Kim, S. -J., & Vihma, T. (2015). The melting Arctic and midlatitude weather patterns: Are they connected? *Journal of Climate*, 28(20), 7917-7932. doi: 10.1175/JCLI-D-14-00822.1
- Park, D. -S. R., Lee, S., & Feldstein, S. B. (2015). Attribution of the recent winter sea-ice decline over the Atlantic sector of the Arctic Ocean." *Journal of Climate*, 28(10), 4027-4033. doi: <http://dx.doi.org/10.1175/JCLI-D-15-0042.1>
- Parkinson, C. L., Cavalieri, D. J., Gloersen, P., Zwally, H. J., & Comiso, J. C. (1999). Arctic sea ice extents, areas, and trends, 1978-1996. *Journal of Geophysical Research*, 104(C9), 20837-20856. doi: 10.1029/1999JC900082
- Peters, D. H. W., Vargin, P., Gabriel, A., Tsvetkova, N., & Yushkov, V. (2010). Tropospheric forcing of the boreal polar vortex splitting in January 2003. *Annales Geophysicae*, 28(11), 2133–2148. <http://doi.org/10.5194/angeo-28-2133-2010>
- Porter, D. F., Cassano, J. J., & Serreze, M. C. (2012). Local and large-scale atmospheric responses to reduced Arctic sea ice and ocean warming in the WRF model. *Journal of Geophysical Research*, 117(D11115). doi: 10.1029/2011JD016969
- Rea, K. J. (n.d.). Nunavut. In *Encyclopædia Britannica online*. Retrieved from <http://www.britannica.com/place/Nunavut>
- Rinke, A., Melsheimer, C., Dethloff, K., & Heygster, G. (2009). Arctic total water vapor: Comparison of regional climate simulations with observations, and simulated decadal trends. *Journal of Hydrometeorology*, 10(1), 113-129. doi: 10.1175/2008JHM970.1
- Saha, S. K., Rinke, A., & Dethloff, K. (2006). Future winter extreme temperature and precipitation events in the Arctic." *Geophysical Research Letters*, 33(15), L15818. doi: 10.1029/2006GL026451
- Saha, S., Moorthi, S., Pan, H. -L., Wu, X., Wang, J., Nadiga, S., . . . Goldberg, M. (2010). The NCEP climate forecast system reanalysis. *Bulletin of the American Meteorological Society*, 91, 1015-1057. doi: 10.1175/2010BAMS3001.2
- Schuenemann, K. C., Cassano, J. J., & Finnis, J. (2009). Synoptic forcing of precipitation over Greenland: Climatology for 1961-99. *Journal of Hydrometeorology*, 10(1), 60-78. doi: 10.1175/2008JHM1014.1
- Screen, J. A. & Simmonds, I. (2010). The central role of diminishing sea ice in recent Arctic temperature amplification. *Nature*, 464(7293). doi: 10.1038/nature09051
- Semmler, T., McGrath, R., & Wang, S. (2012). The impact of Arctic sea ice on the Arctic energy budget and on the climate of the northern mid-latitudes. *Climate Dynamics*, 39(11), 2675-2694. doi: 10.1007/s00382-012-1353-9
- Serreze, M. C. & Barrett, A. P. (2008). The summer cyclone maximum over the central Arctic Ocean. *Journal of Climate*, 21(5), 1048-1065. doi: 10.1175/2007JCLI1810.1
- Serreze, M. C. & Barry, R. G. (2014). *The Arctic Climate System* (2nd ed.). Cambridge, UK: Cambridge University Press.
- Serreze, M. C. & Francis, J. A. (2006). The Arctic amplification debate. *Climatic Change*, 76(3), 241-264. doi: 10.1007/s10584-005-9017-y

- Serreze, M. C., Barrett, A. P., & Stroeve, J. (2012). Recent changes in tropospheric water vapor over the Arctic as assessed from radiosondes and atmospheric reanalyses. *Journal of Geophysical Research Atmospheres*, *117*(D10), 1-22. doi: 10.1029/2011JD017421
- Serreze, M. C., Carse, F., Barry, R. G., & Rogers, J. C. (1997). Icelandic low cyclone activity: Climatological features, linkages with the NAO, and relationships with recent changes in the northern hemisphere circulation. *Journal of Climate*, *10*(3), 453-464. doi: 10.1175/1520-0442(1997)010<0453:ILCACF>2.0.CO;2
- Serreze, M. C., Lynch, A. H., & Clark, M. P. (2001). The Arctic Frontal Zone as seen in the NCEP-NCAR reanalysis. *Journal of Climate*, *14*(7), 1550-1567. doi: [http://dx.doi.org/10.1175/1520-0442\(2001\)014<1550:TAFZAS>2.0.CO;2](http://dx.doi.org/10.1175/1520-0442(2001)014<1550:TAFZAS>2.0.CO;2)
- Shulski, M. & Wendler, G. (2007). *Climate of Alaska*. Fairbanks, AK: University of Alaska Press.
- Simmonds, I. & Keay, K. (2009). Extraordinary September Arctic sea ice reductions and their relationships with storm behavior over 1979-2008. *Geophysical Research Letters*, *36*, L19715. doi: 10.1029/2009GL039810
- Ulbrich, U., Leckebusch, G. C., Grieger, J., Schuster, M., Akperov, M., Bardin, M. Y., . . . The Imilast Team (2013). Are greenhouse gas signals of northern hemisphere winter extra-tropical cyclone activity dependent on the identification and tracking algorithm? *Meteorologische Zeitschrift*, *22*(1), 61-68. doi: 10.1127/0941-2948/2013/0420
- Uppala, S. M., KÅllberg, P. W., Simmons, A. J., Andrae, U., Bechtold, V. D. C., Fiorino, M., . . . Woollen, J. (2005). The ERA-40 re-analysis. *Quarterly Journal of the Royal Meteorological Society*, *131*(612), 2961-3012. doi: 10.1256/qj.04.176
- Wanner, H., Brönnimann, S., Casty, C., Gyalistras, D., Luterbacher, J., Schmutz, C., . . . Xoplaki, E. (2001). North Atlantic oscillation - concepts and studies. *Surveys in Geophysics*, *22*(4), 321-382. doi: 10.1023/A:1014217317898
- Weather Underground. (2011). *Weather history for PAOT - July, 2011* [Data file]. Retrieved from http://www.wunderground.com/history/airport/PAOT/2011/7/23/DailyHistory.html?req_city=Kotzebue&req_state=&req_statename=Alaska&reqdb.zip=&reqdb.magic=&reqdb.wmo=
- Wendler, G., Shulski, M., & Moore, B. (2010). Changes in the climate of the Alaskan north slope and the ice concentration of the adjacent Beaufort Sea. *Theoretical and Applied Climatology*, *99*, 67-74. doi: 10.1007/s00704-009-0127-8
- Yang, D., Goodison, B., Metcalfe, J., Louie, P., Elomaa, E., Hanson, C., . . . Lapin, M. (2001). Compatibility evaluation of national precipitation gage measurements. *Journal of Geophysical Research*, *106*(D2), 1481-1491. doi: 10.1029/2000JD900612
- Zhang, X., Walsh, J. E., Zhang, J., Bhatt, U. S., & Ikeda, M. (2004). Climatology and interannual variability of Arctic cyclone activity: 1948-2002. *Journal of Climate*, *17*(12), 2300-2317. doi: [http://dx.doi.org/10.1175/1520-0442\(2004\)017<2300:CAIVOA>2.0.CO;2](http://dx.doi.org/10.1175/1520-0442(2004)017<2300:CAIVOA>2.0.CO;2)
- Zhao, J., Cao, Y., & Shi, J. (2010). Spatial variation of the Arctic oscillation and its long-term change. *Tellus A*, *62*(5), 661-672. doi: 10.1111/j.1600-0870.2010.00472.x

